

The exact tree-level calculation of the dark photon production in high-energy electron scattering at the CERN SPS

S.N. Gninenko^{1*}, D.V. Kirpichnikov^{1†}, M.M. Kirsanov^{1‡} and N.V. Krasnikov^{1,2§}

¹ Institute for Nuclear Research of the Russian Academy of Sciences,
117312 Moscow, Russia

² Joint Institute for Nuclear Research, 141980 Dubna, Russia

March 13, 2018

Abstract

Dark photon (A') that couples to the standard model fermions via the kinetic mixing with photons and serves as a mediator of dark matter production could be observed in the high-energy electron scattering $e^- + Z \rightarrow e^- + Z + A'$ off nuclei followed by the $A' \rightarrow \textit{invisible}$ decay. We have performed the exact tree-level calculations of the A' production cross sections and implemented them in the program for the full simulation of such events in the experiment NA64 at the CERN SPS. Using simulations results, we study the missing energy signature for the bremsstrahlung $A' \rightarrow \textit{invisible}$ decay that permits the determination of the $\gamma - A'$ mixing strength in a wide, from sub-MeV to sub-GeV, A' mass range. We refine and expand our earlier studies of this signature for discovering A' by including corrections to the previously used calculations based on the improved Weizsaker-Williams approximation, which turn out to be significant. We compare our cross sections values with the results from other calculations and find a good agreement between them. The possibility of future measurements with high-energy electron beams and the sensitivity to A' are briefly discussed.

1 Introduction

At present there are several indications that new physics beyond the Standard Model (SM) exists. The most robust fact is the existence of dark matter (DM), see e.g. [1] -[3]. Among many models of DM, there is a class of models that motivate the existence of light DM with a mass $\lesssim 1$ GeV, for a review see e.g. [4, 5]. In such renormalizable models, there must be a new light vector (scalar) boson which serves as a mediator connecting the visible and DM particles [5]. The most popular realisation of the light DM paradigm is the model with a massive vector boson, called dark photon (A') which interacts with the Standard Model (SM) particles through the mixing with the ordinary photon. The possibility to observe A' through its visible (into SM particles) or invisible (into light

* **e-mail:** sergei.gninenko@cern.ch

† **e-mail:** kirpich@ms2.inr.ac.ru

‡ **e-mail:** mikhail.kirsanov@cern.ch

§ **e-mail:** nikolai.krasnikov@cern.ch

DM particles) decay in accelerator experiments motivate significant efforts devoted to searches for dark photons, for a review see e.g. [5].

The fixed-target experiment NA64 at the CERN SPS [6, 7, 8, 9, 10] is designed to search for A' that can be produced through the mixing with the bremsstrahlung photon from the reaction of high-energy electron scattering off nuclei

$$e^- + Z \rightarrow e^- + Z + A' \tag{1}$$

accompanied by the dominant invisible A' decay. The discussions of the missing energy signature of this process and the distinctive distributions of variables that can be used to distinguish the $A' \rightarrow invisible$ signal from background including the results of the detailed simulation of the detector response to events with and without A' emission and estimates of the efficiency of the signal event selection can be found in Ref. [8]. The evaluation of the sensitivity of the experiment shows that it can probe the still unexplored area of the mixing strength $10^{-6} \lesssim \epsilon \lesssim 10^{-2}$ and masses up to $M_{A'} \lesssim 1$ GeV. In the case of the signal observation, a possibility of determining the A' mass $m_{A'}$ and mixing strength ϵ using the missing energy spectrum shape was also discussed.

The results presented in Ref. [8, 9] were based on the full Monte Carlo simulations obtained by using the improved Weizsaker-Williams (IWW) approximation [11, 12] for the differential cross section calculations of the process (1). Recently, the exact, tree-level (ETL) calculations of the cross sections for the A' production in the reaction (1) performed by Liu et al. were published [13]. It was pointed out that for a certain range of the initial electron beam energy E_0 and the A' mass $m_{A'}$, the A' yield calculated in the IWW framework could differ significantly from the one calculated exactly at tree-level [13]. It is clear that reliable theoretical predictions for the A' yield are essential for a proper interpretation of the experimental results both in case of observation of signal or non-observation. In the latter case they are necessary to obtain robust exclusion limits in the A' parameter space. Therefore, it is instructive to perform an accurate calculation of the A' cross-section based on precise phase space integration over the final state particles in the reaction $e^- Z \rightarrow e^- Z A'$. This provides the main motivation for this work. First, it is crucial to cross-check and confirm the results of Ref. [13], which could be also useful for other dark force experiments planned with electron beams [5]. Second, it is important to implement the ETL cross sections in the NA64 simulation software.

The organisation of the paper is as follows. In Section 2 we present the results for ETL calculations of the cross section relevant for the NA64 experiment and compare them with analogous calculations based on the use of the IWW approximation and with the results of Liu et al. [13]. In Section 3 we implement ETL cross sections for the reaction $e^- + Z \rightarrow e^- + Z + A'$ in the NA64 simulation software and compare obtained results with the previous full simulation calculations based on the use of the IWW approximation. In Section 4 we evaluate the sensitivity in terms of the mixing parameter ϵ of the NA64 experiment to invisibly decaying dark photons in the wide range of A' masses. Section 5 contains concluding remarks.

2 Cross sections

The Lagrangian of the dark sector has the following form

$$\begin{aligned} \mathcal{L} = & -\frac{1}{4}F'_{\mu\nu}F'^{\mu\nu} + \frac{\epsilon}{2}F'_{\mu\nu}F^{\mu\nu} + \frac{m_{A'}^2}{2}A'_\mu A'^\mu \\ & + i\bar{\chi}\gamma^\mu\partial_\mu\chi - m_\chi\bar{\chi}\chi - e_D\bar{\chi}\gamma^\mu A'_\mu\chi, \end{aligned} \tag{2}$$

where A'_μ is a massive Dark photon field which originates from broken $U'(1)$ gauge group, ϵ is the value of the kinetic mixing between SM photon and Dark photon, χ is Dirac spinor which can be

treated as Dark Matter fermions coupled to A'_μ by the coupling constant e_D . The interaction between the Dark photon and SM fermions are described by the following Lagrangian

$$\mathcal{L}_{int} = \epsilon e A'_\mu J_{em}^\mu. \quad (3)$$

The decay rates of invisible and visible decays are given by

$$\begin{aligned} \Gamma(A' \rightarrow \bar{\chi}\chi) &= \frac{\alpha_D}{3} m_{A'} \left(1 + \frac{2m_\chi^2}{m_{A'}^2}\right) \sqrt{1 - \frac{4m_\chi^2}{m_{A'}^2}}, \\ \Gamma(A' \rightarrow e^-e^+) &= \frac{\alpha_{QED}\epsilon^2}{3} m_{A'} \left(1 + \frac{2m_e^2}{m_{A'}^2}\right) \sqrt{1 - \frac{4m_e^2}{m_{A'}^2}}, \end{aligned} \quad (4)$$

where $\alpha_{QED} = e^2/4\pi$, $\alpha_D = e_D^2/4\pi$ and m_e , m_χ are the electron and DM particle masses, respectively. We suppose that the A' lepton decay channel is suppressed, $\Gamma(A' \rightarrow \bar{\chi}\chi) \gg \Gamma(A' \rightarrow e^-e^+)$, and that dark matter invisible decay mode is dominant, i.e. $\Gamma(A' \rightarrow \bar{\chi}\chi)/\Gamma_{tot} \simeq 1$.

2.1 The IWW cross sections

In the IWW approximation the differential and total cross sections for the reaction (1) for $m_{A'} \gg m_e$ can be written as [12]

$$\frac{d\sigma_{WW}^{A'}}{dx} = (4\alpha^3\epsilon^2\chi) \left(m_{A'}^2 \frac{1-x}{x} + m_e^2 x\right)^{-1} \times \left(1 - x + \frac{x^2}{3}\right), \quad (5)$$

$$\sigma_{WW}^{A'} = \frac{4}{3} \frac{\epsilon^2\alpha^3\chi}{m_{A'}^2} \cdot \log \delta_{A'}^{-1}, \quad \delta_{A'} = \max \left[\frac{m_e^2}{m_{A'}^2}, \frac{m_{A'}^2}{E_0^2} \right], \quad (6)$$

where χ is an effective flux of photons

$$\chi = \int_{t_{min}}^{t_{max}} dt \frac{(t - t_{min})}{t^2} [G_2^{\text{el}}(t) + G_2^{\text{inel}}(t)]. \quad (7)$$

and $x = \frac{E_{A'}}{E_o}$. Here $t_{min} = m_{A'}^4/(4E_0^2)$, $t_{max} = m_{A'}^2$ and $G_2^{\text{el}}(t)$, $G_2^{\text{inel}}(t)$ are elastic and inelastic form-factors respectively. For usual energies the elastic form-factor $G_2^{\text{el}}(t)$ dominates. The elastic form-factor can be written as

$$G_2^{\text{el}}(t) = \left(\frac{a^2 t}{1 + a^2 t} \right)^2 \left(\frac{1}{1 + t/d} \right)^2 Z^2, \quad (8)$$

where $a = 111Z^{-1/3}/m_e$ and $d = 0.164 \text{ GeV}^2 A^{-2/3}$. In our case we consider the quasi-elastic reaction (1), so that inelastic nuclear formfactor is not taken into account. Numerically, $\chi = Z^2 \cdot \text{Log}$, where the function Log weakly depends on atomic screening, nuclear size effects and kinematics [11, 12]. For $m_{A'} \leq 500 \text{ MeV}$ $\text{Log} \approx (5 - 10)$.

2.2 The ETL cross sections

In this subsection we closely follow notations of Ref. [13] to derive the production cross-section of the A' beyond the IWW approximation. To begin with we consider kinematic variables of the process

$$e^-(p) + Z(P_i) \rightarrow e^-(p') + N(P_f) + A'(k),$$

here $p = (E_0, \mathbf{p})$ is the 4-momentum of incoming electron, $P_i = (M, 0)$ denotes the Z Nucleus 4-momentum in the initial state, final state Z Nucleus momentum is defined by $P_f = (P_f^0, \mathbf{P}_f)$, the A' -boson momentum is $k = (k_0, \mathbf{k})$ and $p' = (E', \mathbf{p}')$ is the momentum of electron recoil. It is convenient to perform calculation in the frame where vector $\mathbf{V} = \mathbf{p} - \mathbf{k}$ is parallel to z -axis and vector \mathbf{k} is in the xz -plane. We define a 4-momentum transfer to the nucleus as $q = P_i - P_f$. In this frame the polar and axial angles of \mathbf{q} are denoted by θ_q and ϕ_q respectively. In contrast to Ref. [13] we use mostly minus metric, such that $t = -q^2 = |\mathbf{q}|^2 - q_0^2 > 0$. After some algebraic manipulations one can obtain

$$\cos \theta_q = -\frac{|\mathbf{V}|^2 + |\mathbf{q}|^2 + m_e^2 - (E_0 + q_0 - k_0)^2}{2|\mathbf{V}||\mathbf{q}|}, \quad q_0 = -\frac{t}{2M}, \quad |\mathbf{q}| = \sqrt{\frac{t^2}{4M^2} + t}. \quad (9)$$

We assume that nucleus has zero spin [13, 14, 15, 16], as a consequence the photon-nucleus vertex is given by

$$ie\sqrt{G_2^{\text{el}}(t)}(P_i + P_f)_\mu \equiv ie\sqrt{G_2^{\text{el}}(t)}\mathcal{P}_\mu.$$

We also use a convenient designation for the partial energy of A' -boson $x = k_0/E_0$ and for the angle θ between \mathbf{k} and \mathbf{p} .

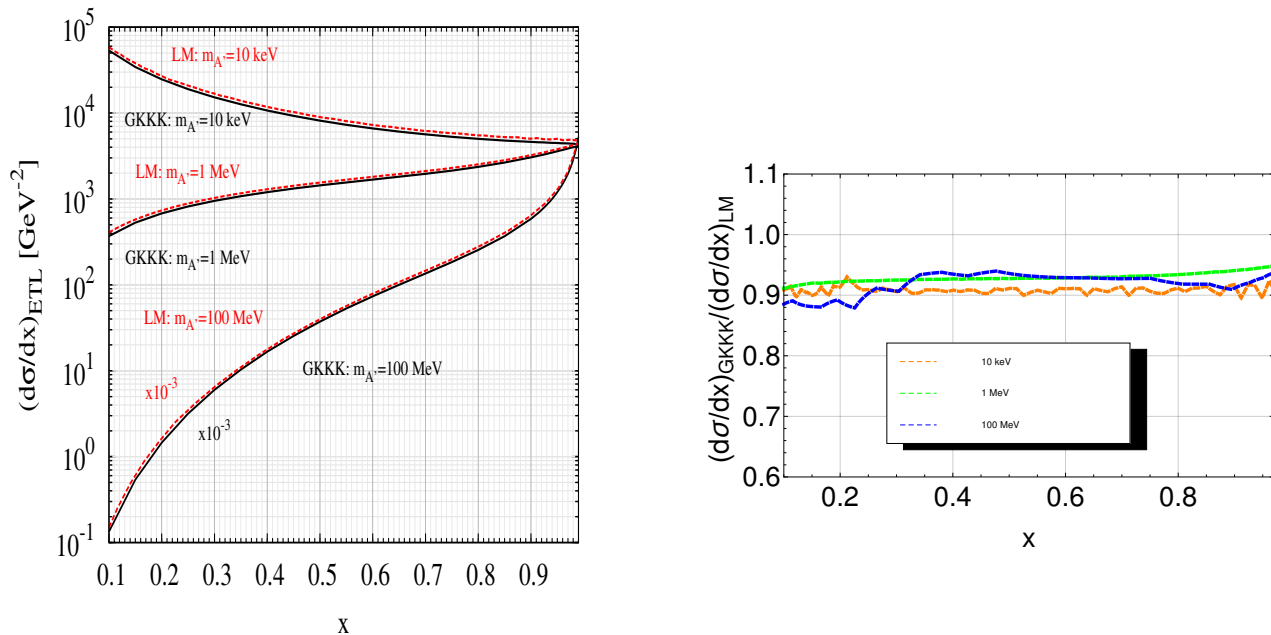


Figure 1: Left panel: Comparison of the values of the differential cross section $(d\sigma/dx)_{\text{ETL}}$ as a function of $x = E_{A'}/E_0$ for various A' masses and mixing strength $\epsilon = 1$ calculated in this work (curves labeled with GKKK) and in Ref. [13] (LM curves). The spectra are normalized to the same number of electron on target. Right panel: ratio of ETL cross-sections shown on the left panel for various masses of dark photon, $10 \text{ keV} < m_{A'} < 100 \text{ MeV}$.

One can express the relevant differential cross-section in the following form [13]

$$\frac{d\sigma}{dx d\cos\theta} = \frac{\epsilon^2 \alpha^3 |\mathbf{k}| E_0}{|\mathbf{p}||\mathbf{k} - \mathbf{p}|} \cdot \int_{t_{\min}}^{t_{\max}} \frac{dt}{t^2} G_2^{\text{el}}(t) \cdot \int_0^{2\pi} \frac{d\phi_q}{2\pi} \frac{|A_X^{2 \rightarrow 3}|^2}{8M^2}, \quad (10)$$

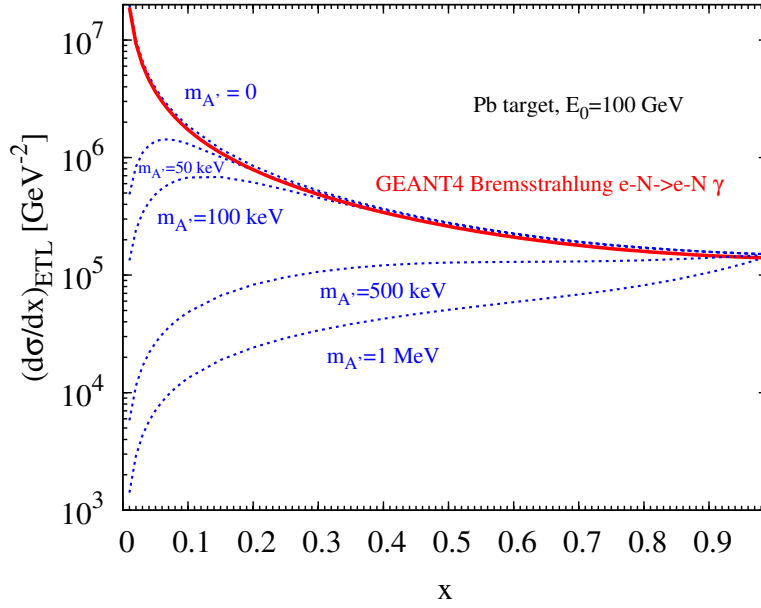


Figure 2: Differential cross-section of A' production as a function of x for various masses $m_{A'} < 1$ MeV and $\epsilon = 1$.

where t_{\min} and t_{\max} are the values of minimum and maximum momentum transfer respectively. The quantities for t_{\min} and t_{\max} are derived explicitly in Ref. [13]. The production amplitude squared for dark photon is given by

$$|A_{A'}^{2 \rightarrow 3}|^2 = \frac{2}{\tilde{s}^2 \tilde{u}^2} \left(2m_e^2 (\mathcal{P}^2 t (\tilde{s} + \tilde{u})^2 - 4((\mathcal{P} \cdot p) \tilde{u} + (\mathcal{P} \cdot p') \tilde{s})^2) + m_{A'}^2 (\mathcal{P}^2 t (\tilde{s} - \tilde{u})^2 - 4((\mathcal{P} \cdot p) \tilde{u} + (\mathcal{P} \cdot p') \tilde{s})^2) + \tilde{s} \tilde{u} (\mathcal{P}^2 ((\tilde{s} + t)^2 + (\tilde{u} + t)^2) - 4t[(\mathcal{P} \cdot p)^2 + (\mathcal{P} \cdot p')^2]) \right), \quad (11)$$

where the mandelstam variables and relevant dot products are

$$\tilde{s} = (p' + k)^2 - m_e^2 = 2(p' \cdot k) + m_{A'}^2, \quad \tilde{u} = (p - k)^2 - m_e^2 = -2(p \cdot k) + m_{A'}^2, \quad (12)$$

$$\mathcal{P}^2 = 4M^2 + t, \quad \mathcal{P} \cdot p = 2ME_0 k_0 - (\tilde{s} + t)/2, \quad \mathcal{P} \cdot p' = 2M(E_0 - k_0) + (\tilde{u} - t)/2. \quad (13)$$

We performed the integration of $|A_{A'}^{2 \rightarrow 3}|^2$ over ϕ_q and found that

$$\int_0^{2\pi} \frac{d\phi}{2\pi} |A_{A'}^{2 \rightarrow 3}|^2 = A_{A'}^{(0)} + Y \cdot A_{A'}^{(1)} + \frac{1}{W^{1/2}} \cdot A_{A'}^{(-1)} + \frac{Y}{W^{3/2}} \cdot A_{A'}^{(-2)}, \quad (14)$$

The relevant functions $A_{A'}^{(i)}$ are given by

$$A_{A'}^{(-2)} = -8M (4E_0^2 M - t(2E_0 + M)) (m_{A'}^2 + 2m_e^2), \quad A_{A'}^{(1)} = \frac{8M^2}{\tilde{u}}, \quad (15)$$

$$A_{A'}^{(-1)} = \frac{8}{\tilde{u}} \left[M^2 (2t\tilde{u} + \tilde{u}^2 + 4E_0^2 (2(x-1)(m_{A'}^2 + 2m_e^2) - t((x-2)x + 2))) + 2t(-m_{A'}^2 + 2m_e^2 + t) \right] - \quad (16)$$

$$-2E_0Mt \left((1-x)\tilde{u} + (x-2)(m_{A'}^2 + 2m_e^2 + t) \right) + t^2 (\tilde{u} - m_{A'}^2) \Big],$$

$$A_{A'}^{(0)} = \frac{8}{\tilde{u}^2} \left[M^2 (2t\tilde{u} + (t - 4E_0^2(x-1)^2)(m_{A'}^2 + 2m_e^2)) + 2E_0Mt (\tilde{u} - (x-1)(m_{A'}^2 + 2m_e^2)) \right], \quad (17)$$

The functions Y and W have the form

$$Y = q^2 + 2q_0E_0 - 2\frac{|\mathbf{q}||\mathbf{p}|}{|\mathbf{V}|}(|\mathbf{p}| - |\mathbf{k}| \cos \theta) \cos \theta_q, \quad W = Y^2 - 4\frac{|\mathbf{q}|^2|\mathbf{p}|^2|\mathbf{k}|^2}{|\mathbf{V}|^2} \sin^2 \theta \sin^2 \theta_q. \quad (18)$$

To derive the total cross-section we integrate (10) over all kinematically allowed variables x and θ .

In the numerical estimates we use the electron energy $E = 100$ GeV and the lead target with $Z = 82$ relevant for the NA64 experiment. In Fig.1 we present the results of our numeric calculations for the differential and total cross sections. In the left panel of Fig. 1, we also show the detailed comparison of the A' differential cross sections calculated at the ETL level in this work, with the one calculated in Ref.[13]. The comparison is made for the case of the aluminium target, A' masses in the range from 10 keV to 100 MeV and the beam energy $E_0 = 20$ GeV. In order to better illustrate the comparison between the two calculations, in Table 1 we also show the difference between the values of the total cross sections calculated for the aluminium target and beam energy 20 GeV using the results of Ref.[13]. One can see that for x values in the range $0.5 < x < 1$ relevant for NA64, the difference is within $\lesssim 10\%$ for the full mass range. The difference

$$\Delta_0 = [(d\sigma/dx)_{LM} - (d\sigma/dx)_{GKKK}]/(d\sigma/dx)_{LM}$$

between the differential cross sections for x values $0.5 < x < 1$ is varying in the range $6.5\% \lesssim \Delta_0 \lesssim 9.2\%$ for the mass range $10 \text{ keV} \lesssim m_{A'} \lesssim 100 \text{ MeV}$. The observed difference can be interpreted as due to the accuracy of numerical integration of the A' production cross section, the figure digitization accuracy [17] and also due to the difference in the nuclei form-factors used in calculations. It can be conservatively accounted for as additional systematic uncertainty in the evaluation of the A' yield.

$m_{A'}$	10 keV	1 MeV	100 MeV
$\sigma_{tot}^{GKKK} [\text{GeV}^{-2}]$	2668.78	1105.13	0.212
$\sigma_{tot}^{LM} [\text{GeV}^{-2}]$	2938.63	1216.97	0.230
$(\sigma_{tot}^{LM} - \sigma_{tot}^{GKKK})/\sigma_{tot}^{LM}$	9.2 %	6.5 %	7.6 %

Table 1: Comparison of the total cross-sections with those from Ref.[13] integrated in the region $0.5 < x < 1$ for the Al target, $\epsilon = 1$ and $E_0 = 20$ GeV.

Independent cross-check has been made by comparing the brems-spectra obtained with the Geant4 package [18] and calculated with the integration code. The comparison (see Fig. 2) shows that the relative difference between Geant4 and our calculations does not exceed 2-8 % for the full brems. photon energy range.

2.3 Infrared divergences and applicability of the cross sections to the mass region $m_{A'} < 1$ MeV.

As is well known, the infrared divergences arise in some theories (QED, QCD) with massless particles. There are two types of infrared singularities - collinear singularities and soft photon(gluon) singularities. In QED with nonzero electron mass there are no collinear singularities and only soft photon

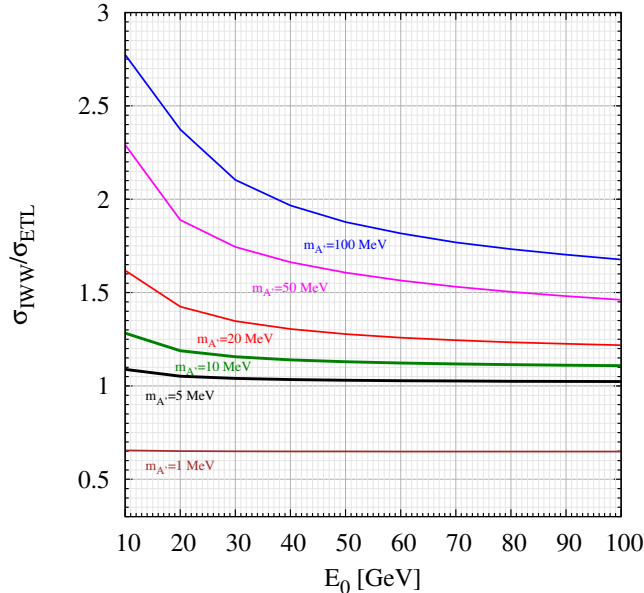


Figure 3: The ratio $\sigma_{IWW}/\sigma_{ETL}$ as a function of electron beam energy E_0 for various masses $m_{A'}$.

singularities exist. To understand the origin of infrared singularities let us consider the expression (6) for the differential cross section. For massless electron $m_e = 0$ we have $\frac{d\sigma_{IWWA'}}{dx} \sim \frac{1}{(1-x)m_{A'}^2}$ at $1-x \ll 1$ that corresponds to the collinear singularity at $x = 1$. Nonzero electron mass regulates the collinear infrared singularity. For massless A' boson we have the situation with soft dark photon infrared divergences similar to standard QED, namely $\frac{d\sigma_{IWWA'}}{dx} \sim \frac{1}{xm_e^2}$ at $x \approx 0$. So the differential cross section is infrared divergent for massless A' in the limit $E_A \rightarrow 0$. Note that according to Bloch-Nordsik theorem in QED with finite electron masses it is sufficient to sum over degenerate final states, i.e. soft photons in final states to cancel infrared divergences. For massive A' dark photon we have no infrared divergences at all as follows from the expression (5) for the differential cross section¹. Moreover, in the search for dark photon A' in NA64 we use rather high cut $E_{A'} > \frac{E_0}{2} = 50 \text{ GeV}$, i.e. $x > 0.5$ ².

Let us stress that the use of this cut means that even for massless A' boson we escape the infrared divergences arising at $x \ll 1$, therefore our calculations for the differential cross sections and the total cross section $\int_{x=0.5}^{x=1} dx \frac{d\sigma_{IWWA'}}{dx}$ are infrared safe and reliable also for the mass range $m_{A'} < 1 \text{ MeV}$. Moreover, the standard QED condition $\frac{\alpha}{\pi} \epsilon^2 \log^2\left(\frac{t}{m_e^2}\right) \ll 1$ for the applicability of the perturbation theory works in our case even for $\epsilon = 1$.

¹The introduction of nonzero photon mass is often used as infrared regularization in QED.

²The use of this cut means that we consider the phase space region only with relativistic A' dark photon

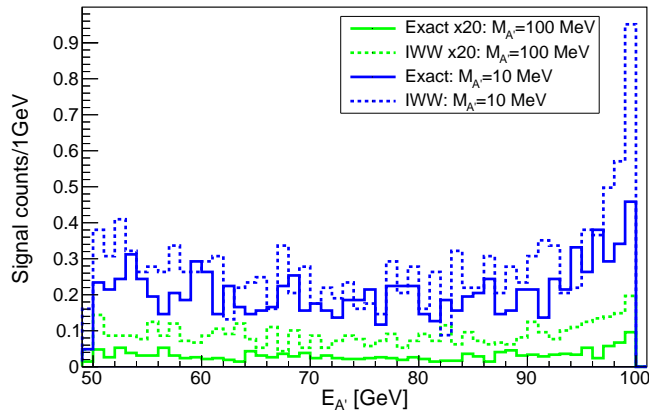


Figure 4: Number of signal events at NA64 as a function of Dark Photon energy $E_{A'}$ for $m_{A'} = 10$ MeV and $m_{A'} = 100$ MeV.

3 Signal event simulation

3.1 MC simulation of missing energy events.

First we summarise the main features of MC simulation of the A' production in NA64. The number of A' bosons produced by electrons in the active target is given by

$$N_{A'} = \frac{1}{A} \times N_{\text{EOT}} \times \rho \times N_A \times \sum_i \sigma_{\text{tot}}^{A'}(E_e^i) \times \Delta L_i, \quad (19)$$

where A is the atomic weight, N_A is Avogadro's number, N_{EOT} is the number of electrons on target, ρ is the target density, E_e^i is the electron energy at the i th step in the target, ΔL_i is step length of electron path and $\sigma_{\text{tot}}^{A'}$ is the total cross-section for the A' production in the $e^- Z \rightarrow e^- Z A'$ reaction. The summation in (19) is performed by simulating the electromagnetic shower development from electrons in the active target with **GEANT4**. In the real simulation of signal samples, at each simulation step the following actions are made

- we randomly sample the variable u_1 uniformly distributed in the range $[0, 1]$, if u_1 is smaller than the A' emission probability

$$P_{\text{emission}} = \rho N_A \sigma_{\text{tot}}^{A'} \Delta L_i / A,$$

then the emission of A' is accepted,

- for each emitted A' we randomly generate the values of x , $\cos \theta$ and the azimuthal angle ϕ from the kinematically allowed region and then by using the Von Neuman rejection sampling we accept x , $\cos \theta$ and ϕ as a signal event values of A' emission to calculate 4-momentum of the Dark Photon.

Fig. 4 shows the relevant spectra of Dark Photon for Pb target, $\epsilon = 10^{-4}$ and $EOT = 10^{11}$. These spectra correspond to missing energy distribution of electron beam at NA64.

3.2 Simulation with the ETL cross sections

Now let us describe the implementation of exact total cross-section formula into **GEANT4** numerical simulation of A' production. From (19) follows that the yield of dark photon is proportional to the total cross-section. Therefore, in order to have the A' yield corresponding to ETL instead of the one calculated with WW approximation in the **GEANT 4** full simulation we define the following ratio (K-factor):

$$K(m_{A'}, E_0, Z, A) = \sigma_{\text{WW}}^{A'}/\sigma_{\text{ETL}}^{A'}, \quad (20)$$

which represents the overall correction to the cross-section (6) calculated in the IWW approach. In Fig. 3 we show K -factors as a function of the electron beam energy E_0 for various $m_{A'}$. For heavy nuclei K depends rather weakly on Z and A , e.g. for the W and Pb nuclei the difference is a few %. In our **GEANT4** MC simulations of the A' production we use tabulated K -factors. From Fig. 3 and Table 2 one can see that σ_{ETL} cross-section of A' production is smaller by a factor of ~ 1.67 than the corresponding σ_{IWW} cross-section obtained in IWW approach for $m_{A'} = 100$ MeV and $E_0 = 100$ GeV. On the other hand, σ_{ETL} exceeds σ_{WW} for the Dark Photon masses $m_{A'}$ below 5 MeV. This means that the sensitivity to the mixing strength ϵ [8] for this mass region becomes better.

$m_{A'}, \text{ MeV}$	1	5	10	20	50	100
$\sigma_{\text{IWW}}/\sigma_{\text{ETL}}, E_0 = 100 \text{ GeV}$	0.648	1.023	1.10	1.21	1.46	1.67
$\epsilon_{\text{ETL}}^2/\epsilon_{\text{IWW}}^2$	0.85	1.14	1.42	1.78	1.90	2.32

Table 2: The ratio $\sigma_{\text{IWW}}/\sigma_{\text{ETL}}$ for various masses $m_{A'}$ for the electron beam energy $E_0 = 100$ GeV. The ratio of limits on mixing ϵ^2 obtained with a full MC simulations for the ETL and IWW cross sections, as discussed in Sec. 4, is also shown for different A' masses.

4 Expected bounds on mixing strength

In this section we estimate the expected sensitivity of the NA64 experiment to the mixing strength ϵ with the **GEANT4** MC simulation. We calculate the missing energy spectra of the NA64 and impose the cut $E_{\text{miss}} > 0.5E_0$. By using Eq.(19) and Eq.(20) and the relation $n_{A'}^{90\%} > n_{A'}$, where $n_{A'}^{90\%} = 2.3$ is the Poisson 90% CL upper limit on the number of Dark Photon production events for the background free case and no signal, we obtain the expected limits on $m_{A'}$ and ϵ shown in Fig. 5. Taking into account discussion in Section 2.3, the bounds are obtained for the mass range $10^{-5} - 1$ GeV and for the total number of 100 GeV electrons on target $n_{\text{EOT}} = 4 \times 10^{10}, 4 \times 10^{11},$ and 4×10^{12} . It is assumed that the A' decays mainly into invisible final states of the Dark sector, $A' \rightarrow \chi\chi$. The obtained results show that the expected sensitivity of the NA64 experiment potentially allows to test the still unexplored area of the mixing strength $10^{-6} \lesssim \epsilon \lesssim 10^{-2}$ and masses from $m_{A'} \lesssim 1$ GeV up to a very small values $\ll 1$ MeV.

5 Summary

Here we briefly summarise the main improvements achieved in this work with respect to our previous paper [8], as well as the recent work on cross section calculations carried out in Ref.[13]. We have studied the missing energy signature of the dark photon production in the reaction (1) in the experiment NA64 at the CERN SPS. For this study we performed the exact tree-level calculations of the

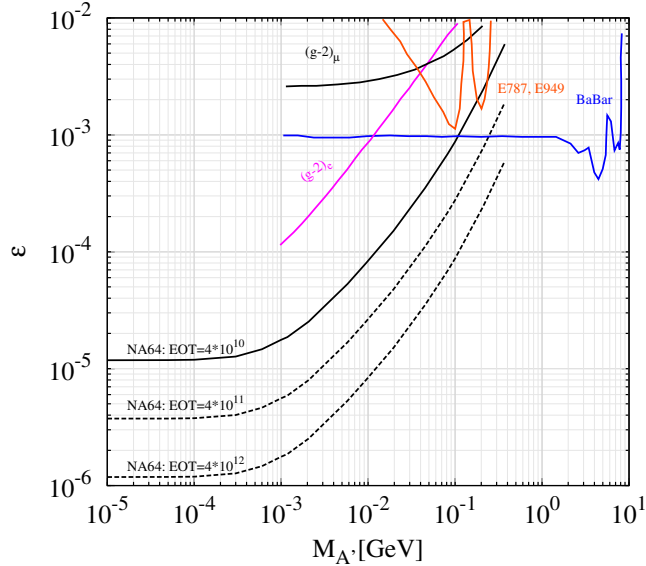


Figure 5: Expected upper limits on the mixing ϵ vs $m_{A'}$ for invisibly decaying A' calculated for the ECAL target [7], $E_0 = 100$ GeV, and the missing energy $E_{miss} > 0.5E_0$ for different numbers of electron on target (EOT). Constraints from the E787 and E949 [20, 21] and BaBar [22] experiments, as well as the muon α_μ favored area are also shown. Here, $\alpha_\mu = \frac{g_\mu - 2}{2}$, see [5].

A' production cross sections and implemented them into the GEANT4 based simulation program of the NA64 detector. We cross-checked our results with the results of Ref.[13] and found that they are in a quite good agreement for the wide mass range. We believe that the error of the estimate of the total cross sections in the sub-MeV - sub-GeV mass range obtained in these two works hardly exceeds a few %. This small difference can be used as a systematic uncertainty of the A' yield. For a realistic study of the expected sensitivity of the NA64 experiment we made the following improvements: we implemented the ETL A' cross sections in the GEANT4 simulation package and performed the full simulation of the detector response to the $A' \rightarrow invisible$ signal events in a wide mass region. We have evaluated the expected sensitivity of the NA64 experiment and have shown that it potentially allows to probe the still unexplored area on the $m_{A'}, \epsilon$ plane for $10^{-6} \lesssim \epsilon \lesssim 10^{-2}$ and a wide A' mass range including the sub-MeV region.

Acknowledgments

We would like to thank the members of the NA64 Collaboration for numerous discussions. D.K. would like to thank I. Karpikov and K. Astapov for fruitful discussion. The work of D.K. on simulations of signal events has been supported by the RSF grant 14-22-00161.

References

- [1] As a review, see for example:
S.Profumo, TASI 2012 lectures on astrophysical probes of dark matter, arXiv:1301.0952.

- [2] As a review, see for example:
S.Dodelson, “Modern cosmology”, Amsterdam, Netherlands: Academic Press(2003) 440 p.
- [3] As a recent review, see for example:
G.Arcadi et al., arXiv:1703.07364(2017).
- [4] C.Boehm, T.Ensclin and J.Silk, J.Phys. **G30** (2004) 279;
G.Boehm and P.Fayet, Nucl.Phys. **B683** (2004) 219.
- [5] As a review, see:
J.Alexander et al., arXiv:1608.08632 (2016).
- [6] S. N. Gninenko, Phys. Rev. D **89** (2014) 7, 075008
- [7] S. Andreas *et al.*, “Proposal for an Experiment to Search for Light Dark Matter at the SPS,” arXiv:1312.3309 [hep-ex].
- [8] S. N. Gninenko, N. V. Krasnikov, M. M. Kirsanov and D. V. Kirpichnikov, Phys. Rev. D **94**, no. 9, 095025 (2016) doi:10.1103/PhysRevD.94.095025 [arXiv:1604.08432 [hep-ph]].
- [9] D. Banerjee *et al.* [NA64 Collaboration], Phys. Rev. Lett. **118**, 011802 (2017).
- [10] D. Banerjee *et al.* [NA64 Collaboration], arXiv:1710.00971 [hep-ex].
- [11] Y. S. Tsai, Rev. Mod. Phys. **46**, 815 (1974) Erratum: [Rev. Mod. Phys. **49**, 521 (1977)]. doi:10.1103/RevModPhys.46.815, 10.1103/RevModPhys.49.421
- [12] J. D. Bjorken, R. Essig, P. Schuster and N. Toro, Phys. Rev. D **80**, 075018 (2009) doi:10.1103/PhysRevD.80.075018 [arXiv:0906.0580 [hep-ph]].
- [13] Y. S. Liu and G. A. Miller, Phys. Rev. D **96**, no. 1, 016004 (2017) doi:10.1103/PhysRevD.96.016004 [arXiv:1705.01633 [hep-ph]].
- [14] Y. S. Liu, D. McKeen and G. A. Miller, Phys. Rev. D **95**, no. 3, 036010 (2017) doi:10.1103/PhysRevD.95.036010 [arXiv:1609.06781 [hep-ph]].
- [15] T. Beranek and M. Vanderhaeghen, Phys. Rev. D **89**, no. 5, 055006 (2014) doi:10.1103/PhysRevD.89.055006 [arXiv:1311.5104 [hep-ph]].
- [16] T. Beranek, H. Merkel and M. Vanderhaeghen, Phys. Rev. D **88**, 015032 (2013) doi:10.1103/PhysRevD.88.015032 [arXiv:1303.2540 [hep-ph]].
- [17] A. Rohatgi, ”WebPlotDigitizer” v4, <https://automeris.io/WebPlotDigitizer/>
- [18] S. Agostinelli *et al.* [GEANT4 Collaboration], “GEANT4: A Simulation toolkit,” Nucl. Instrum. Meth. A **506**, 250 (2003).
- [19] J. Allison *et al.*, “GEANT4 developments and applications,” IEEE Trans. Nucl. Sci. **53**, 270 (2006).
- [20] H. Davoudiasl, H. S. Lee and W. J. Marciano, “Muon g_2 , rare kaon decays, and parity violation from dark bosons,” Phys. Rev. D **89**, 095006 (2014).
- [21] R. Essig, J. Mardon, M. Papucci, T. Volansky and Y. M. Zhong, “Constraining Light Dark Matter with Low-Energy e^+e^- Colliders,” JHEP **1311**, 167 (2013).

[22] J. P. Lees *et al.* [BaBar Collaboration], “Search for invisible decays of a dark photon produced in e^+e^- collisions at BaBar,” arXiv:1702.03327 [hep-ex].